

SCIENTIFIC REPORTS



OPEN

Inhibition of Calpains Protects Mn-Induced Neurotransmitter release disorders in Synaptosomes from Mice: Involvement of SNARE Complex and Synaptic Vesicle Fusion

Can Wang, Bin Xu, Zhuo Ma, Chang Liu, Yu Deng, Wei Liu & Zhao-Fa Xu

Overexposure to manganese (Mn) could disrupt neurotransmitter release via influencing the formation of SNARE complex, but the underlying mechanisms are still unclear. A previous study demonstrated that SNAP-25 is one of substrate of calpains. The current study investigated whether calpains were involved in Mn-induced disorder of SNARE complex. After mice were treated with Mn for 24 days, Mn deposition increased significantly in basal nuclei in Mn-treated and calpeptin pre-treated groups. Behaviorally, less time spent in the center of the area and decreased average velocity significantly in an open field test after 24 days of Mn exposure. With the increase in MnCl₂ dosage, intracellular Ca²⁺ increased significantly, but pretreatment with calpeptin caused a dose-dependent decrease in calpains activity. There were fragments of N-terminal of SNAP-25 protein appearance in Mn-treated groups, but it is decreased with pretreatment of calpeptin. FM1-43-labeled synaptic vesicles also provided evidence that the treatment with Mn resulted in increasing first and then decreasing, which was consistent with Glu release and the 80 kDa protein levels of SNARE complexes. In summary, Mn induced the disorder of neurotransmitter release through influencing the formation of SNARE complex via cleaving SNAP-25 by overactivation of calpains *in vivo*.

Manganese (Mn) is an essential trace element that is required for maintaining proper function and regulation of numerous biochemical and cellular reactions, it also functions as a cofactor for multiple enzymes¹. Despite its essentiality, at excessive levels Mn is toxic to the central nervous system (CNS)². Mn is not only a common industrial toxicant but an environmental pollutant. Occupational exposure to Mn has been recognized as a health hazard for miners, welders, ferroalloy workers, battery manufacturers and car mechanics³. Mn is also a component of an antiknock gasoline additive, known as methylcyclopentadienyl Mn tricarbonyl (MMT), and combustion results in release of Mn phosphates into the ambient air⁴. Mn is transported to the CNS either as a free ion or as a non-specific protein-bound species and accumulated in striatum, globus pallidus (GP) and the substantia nigra (SN)⁵. Overexposure to Mn from environmental sources can result in a condition known as manganism. Although oxidative stress, energy failure, and mitochondrial dysfunction have been actively investigated as neurotoxic mechanisms of Mn over the past two decades^{6,7}, emerging evidence indicates that disturbance of neurotransmitter release is also one of the important cellular and molecular correlates of neurodegenerative diseases resulting from chronic Mn exposure⁸.

A previous study demonstrated that manganese released into the synaptic cleft may influence synaptic neurotransmission, the levels of glutamate (Glu) and γ -aminobutyric acid (GABA) in the rat hippocampus, were dose-dependently decreased during treatment with manganese⁹. Several studies have established the propensity

Department of Environmental Health, School of Public Health, China Medical University, Shenyang, 110122, People's Republic of China. Correspondence and requests for materials should be addressed to B.X. (email: bxu10@cmu.edu.cn)

of Mn to disrupt Glu transporting systems, thus impairing components of the Gln/Glu- γ -aminobutyric acid cycle and leading to both a reduction in Glu uptake and elevation in extracellular Glu level¹⁰. Mechanisms of Mn disrupting neurotransmitter release are complicated and not firmly established. Therefore, understanding the exact molecular mechanisms of Mn disrupting neurotransmitter release may play a key role linking the complicated neurobehavioral deficits observe following Mn exposure.

SNAREs (soluble N-ethylmaleimidesensitive fusion protein attachment protein receptors) and associated proteins play critical roles in mediating neurotransmitter release¹¹. The SNARE complex consists of three components. The vesicle-associated membrane protein 2 (VAMP-2/synaptobrevin) is a 116-amino acid protein anchored in the vesicle membrane by a single transmembrane domain. Syntaxin 1 is correspondingly anchored in the plasma membrane via a single transmembrane helix. The third component, SNAP-25, has lipid anchors in the plasma membrane¹². SNARE proteins function in fusion by a cycle of assembly into complexes that fuel fusion, and disassembly of the complexes by NSF (N-ethylmaleimide sensitive factor) and SNAPs (soluble NSF-attachment proteins) that makes SNARE proteins available again for another round of fusion¹³. Our previous study had shown that Mn disturbed the expression and interaction of SNARE complex associated proteins and resulted in a decrease of protein expression of SNAP-25 in primary cultured neurons¹⁴, its mechanism needed to further study.

The mechanisms governing the proteolytic cleavage of SNAP-25 are not completely clarified, but a potential candidate protease is calpains. It belongs to a family of calcium-dependent, non-lysosomal, neutral, cysteine proteases, which cleave several cytosolic, membrane or cytoskeleton-associated proteins, seems to play an important role in synaptic plasticity¹⁵. Proteolysis by calpains is likely to change the integrity, localization, and/or activity of endogenous proteins, and results in either the activation or the inhibition of substrate functions. Recent data suggested that the component of the SNARE proteins SNAP-25 was substrates of members of the calpains family in neurons, and calpains may play an important role in the long-lasting regulation of synaptic vesicle fusion by suppressing neurotransmitter release, possibly through the proteolytic cleavage of SNAP-25¹⁶.

Although several studies have reported that Mn could disorder the formation of SNARE complex, little data exist on calpains involved in Mn-induced cleavage of SNAP-25, information that is critical for more fully evaluating the Mn-induced neurotoxicity. Therefore, in order to verify our speculation, calpeptin, an inhibitor of calpains, was being used in this study. We found that calpeptin could relieve Mn-induced SNARE complex formation disorders.

Results

Manganese concentrations and behavioral activity. With the increase of MnCl₂ dosage, there were significant increase in total Mn level in basal nuclei of 50 and 100 μ mol/kg MnCl₂-exposed mice (0.476 ± 0.133 and 0.555 ± 0.127 μ g/g, respectively, $P < 0.01$) compared with control group, the same to the three calpeptin pre-treated groups (Fig. 1A). Behavioral measures were assessed at 8, 16 and 24 days during administration, we found that with increased Mn concentrations, mice were less active and spend less time in the center area, or take longer to initially explore the center area were considered to be displaying emotional alterations. Moreover, Mice in 100 μ mol/kg MnCl₂-exposed group exhibited a significant decrease in locomotor activity during exploration period of the open field test on the 24th day. Specifically, the average velocity was decreased by 53.3% ($P < 0.01$) and the time in the center area was decreased by 35.97% ($P < 0.05$) significantly. The total distance traveled have no significant change but it was decreased visibly. However, 25 and 50 μ mol/kg MnCl₂-exposed mice and all calpeptin pre-treated mice did not show any signs of abnormal behavioral activity at the end of the test (data not shown) (Fig. 1B). There was no significant difference between each group on the 8th day and the 16th day results. And There was no difference between female and male mice.

Mn disrupted synapse structure and numbers of synaptic vesicles. Pathological features of synapse ultrastructure and the numbers of synaptic vesicles were observed with Transmission Electron Microscopy (TEM). In the control group, normal synapse ultrastructure was observed in the basal nuclei: a clear synaptic cleft and less postsynaptic density (PSD), and certain numbers of synaptic vesicles in the presynaptic membrane (Fig. 2a). However, with the increase of administered-MnCl₂ dosage, the number of synaptic vesicles decreased, the thickness of PSD in the synapses increased, and the synaptic cleft became blurred (Fig. 2b–d). In the calpeptin control group, the pathological features of synapses are similar to the control group (Fig. 2e). In the calpeptin pre-treated groups, the number of synaptic vesicles increased, the thickness of PSD in the synapses decreased, and the synaptic cleft became cleared with the increase of calpeptin pre-treat dosage (Fig. 2f–h).

Effects of Mn and calpeptin pretreatment on intracellular Ca²⁺ and calpains activity in mice basal nuclei. Calpains are intracellular calcium-dependent proteases. To examine whether Mn affects calpains activity, we first measured the change of intracellular Ca²⁺ using the Ca²⁺ indicator Fura-2 AM. Treatment of mice with 50 and 100 μ mol/kg MnCl₂ resulted in a significant increase in [Ca²⁺]_i (2.69- and 3.31-fold of control respectively, $P < 0.01$, Fig. 3A). [Ca²⁺]_i was not significantly different in mice pretreated with calpeptin compared with 100 μ mol/kg MnCl₂-treated group, which were still higher than those in the absolute controls (Fig. 3A). Similar to the increase in [Ca²⁺]_i, treatment with 50 and 100 μ mol/kg MnCl₂ also caused a significant increase in calpains activity compared with control (2.3- and 3.8-fold of control, respectively, $P < 0.01$, Fig. 3B). However, calpains activity decreased by 63.31% in mice treated with 100 μ g/kg calpeptin alone compared with the controls ($P < 0.05$). Pretreatment with calpeptin caused a dose-dependent decrease in calpains activity, with the maximum decrease in the mice pretreated with 50 and 100 μ g/kg calpeptin (31.19% and 61.66% respectively, $P < 0.01$, Fig. 3B), but calpains activity was still higher than those in the absolute controls. These data suggested that calpeptin could inhibit the activity of calpains. However, there was no effect on [Ca²⁺]_i.

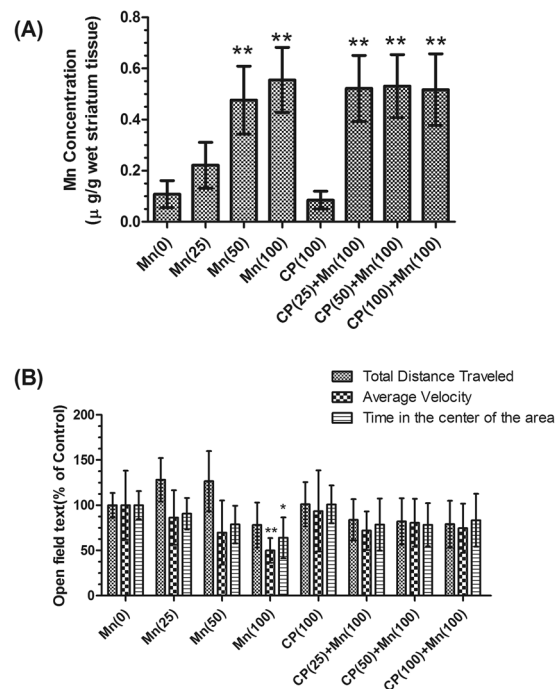


Figure 1. Manganese concentrations of mice basal nuclei and behavioral activity of mice on the 24th day after MnCl_2 -exposed. **(A)** Total Mn levels in basal nuclei of mice. Mice were intraperitoneally (i.p.) treated with physiological saline as control group and MnCl_2 (25, 50, 100 $\mu\text{mol/kg}$) as MnCl_2 -exposed groups, subcutaneously (s.c.) pre-treated with 100 $\mu\text{g/kg}$ calpeptin as calpeptin control group and calpeptin (25, 50, 100 $\mu\text{g/kg}$) accompany with 100 $\mu\text{mol/kg}$ MnCl_2 for 24 days, and 24 h after treatment was finished the basal nuclei were isolated. **(B)** Behavior in an open field test on the 24th day after MnCl_2 -exposed. Mice were placed in the center of the area for 2 min to acclimatization then recorded for 5 min. The total distance traveled, average velocity and time in the inner central zone were measured respectively. The values are expressed as means \pm S.D., $n = 6$. * $P < 0.05$ and ** $P < 0.01$ significantly different from control group; # $P < 0.05$, significantly different from 100 $\mu\text{mol/kg}$ MnCl_2 -treated group.

Effects of Mn and calpeptin pretreatment on the release of neurotransmitters and synaptic vesicle fusion in synaptosomes. To examine the effect of manganese on the neurotransmitters release, endogenous Glu and GABA release in synaptosomes was measured by High Performance Liquid Chromatography (HPLC), with the increase of administered- MnCl_2 dosage, Glu released increased in the 25 and 50 $\mu\text{mol/kg}$ MnCl_2 -treated groups (1.40- and 1.47-fold of control group respectively, $P < 0.01$, Fig. 4A), and decreased by 29.62% in the 100 $\mu\text{mol/kg}$ MnCl_2 -treated group ($P < 0.05$, Fig. 4A). GABA released was decreased sostenuto, it's significantly in 50 and 100 $\mu\text{mol/kg}$ MnCl_2 -treated groups (24.88% and 41.67% of control, $P < 0.05$ and $P < 0.01$, respectively, Fig. 4A). Pretreatment with 100 $\mu\text{mol/kg}$ calpeptin caused an increase in GABA released (1.35-fold of 100 $\mu\text{mol/kg}$ MnCl_2 -treated group, $P < 0.05$, Fig. 4A). To confirm that Mn affects neurotransmitter release, we examined the influence of Mn on KCl-triggered exocytosis by assaying the rate of destaining (loss of FM1-43 fluorescence intensity). It has shown that the fluorescence intensity of before and after KCl-evoked significantly increased in the 50 $\mu\text{mol/kg}$ MnCl_2 -treated group (1.37-fold of control, $P < 0.01$, Fig. 4B), but decreased by 35.82% ($P < 0.01$) in the 100 $\mu\text{mol/kg}$ MnCl_2 -treated group (Fig. 4B). Pretreatment with 100 $\mu\text{g/kg}$ calpeptin caused a significant increase in FM1-43 dye release compared with 100 $\mu\text{mol/kg}$ MnCl_2 -treated group (1.39-fold of 100 $\mu\text{mol/kg}$ MnCl_2 -treated group, $P < 0.05$, Fig. 4B).

Effects of Mn and calpeptin pretreatment on the expression of SNARE complex associated proteins. To investigate the molecular changes that could account for the neurotransmitter release disorders induced by Mn, we first measured the expression of the three presynaptic proteins (Syntaxin 1, SNAP-25 and VAMP-2) forming the SNARE core complex that mediates synaptic exocytosis. As shown in Fig. 5A, real-time PCR analysis showed that the expression of VAMP-2 mRNA significantly increased in a dosage-dependent manner, with the maximum increase in 100 $\mu\text{mol/kg}$ MnCl_2 -treated group (1.40-fold of control, $P < 0.05$). Exposure of the mice to Mn also resulted in a marked decrease in the mRNA expression of SNAP-25 in 50 and 100 $\mu\text{mol/kg}$ MnCl_2 -treated groups (30.44% and 35.12% respectively, $P < 0.05$). However, the mRNA expression of Syntaxin 1 did not significantly change in MnCl_2 -treated groups compared with control group, in addition, the mRNA expression of Syntaxin 1, SNAP25 and VAMP2 did not significantly change in calpeptin pre-treated groups compared with 100 $\mu\text{mol/kg}$ MnCl_2 -treated group.

As shown in Fig. 5C, exposure of the mice to MnCl_2 also resulted in a marked increase in the expression of VAMP-2 protein in 50 and 100 $\mu\text{mol/kg}$ MnCl_2 -treated groups (1.67-, 2.08-fold of control, $P < 0.05$, $P < 0.01$, respectively). The analysis of SNAP-25 by using two different antibodies: a monoclonal antibody directed against

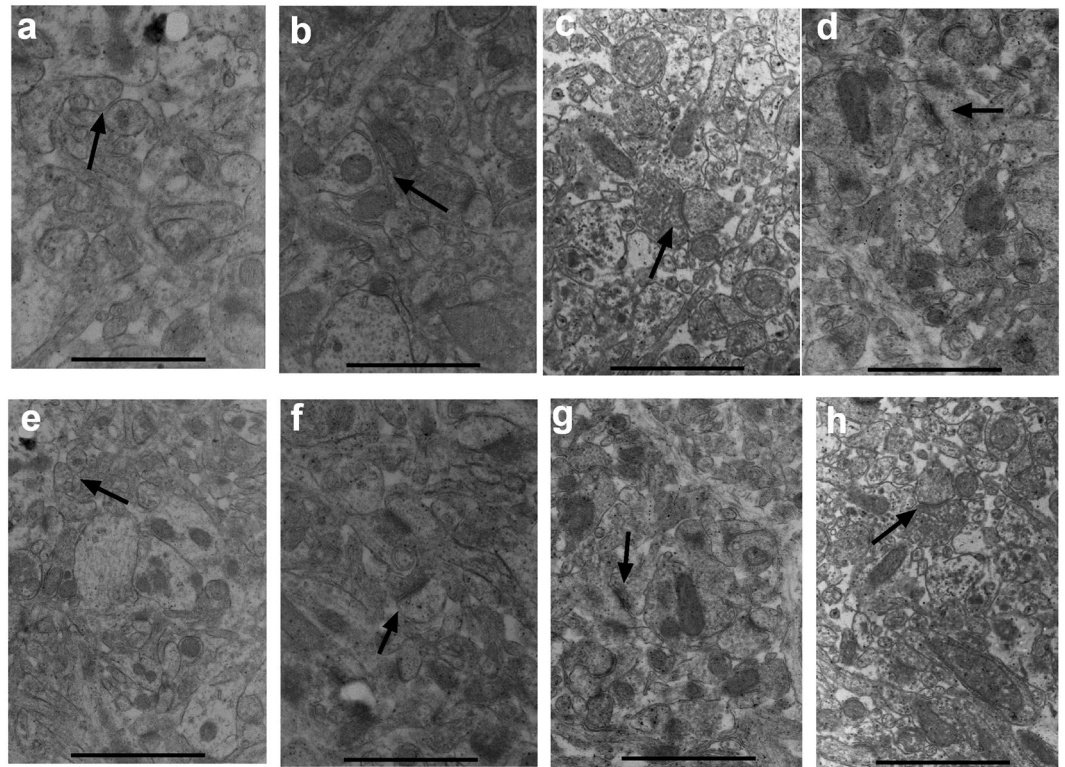


Figure 2. Transmission electron microscopy of synapse ultrastructure and numbers of synaptic vesicles, note the postsynaptic density (arrows). (a) synapse of control group, (b) 25 $\mu\text{mol/kg}$ MnCl_2 -treated group, (c) 50 $\mu\text{mol/kg}$ MnCl_2 -treated group, (d) 100 $\mu\text{mol/kg}$ MnCl_2 -treated group, (e) calpeptin control group, (f) 25 $\mu\text{g/kg}$ calpeptin pre-treated group, (g) 50 $\mu\text{g/kg}$ calpeptin pre-treated group, (h) 100 $\mu\text{g/kg}$ calpeptin pre-treated group. Magnification: $\times 10000$; Scale bars represent 500 nm.

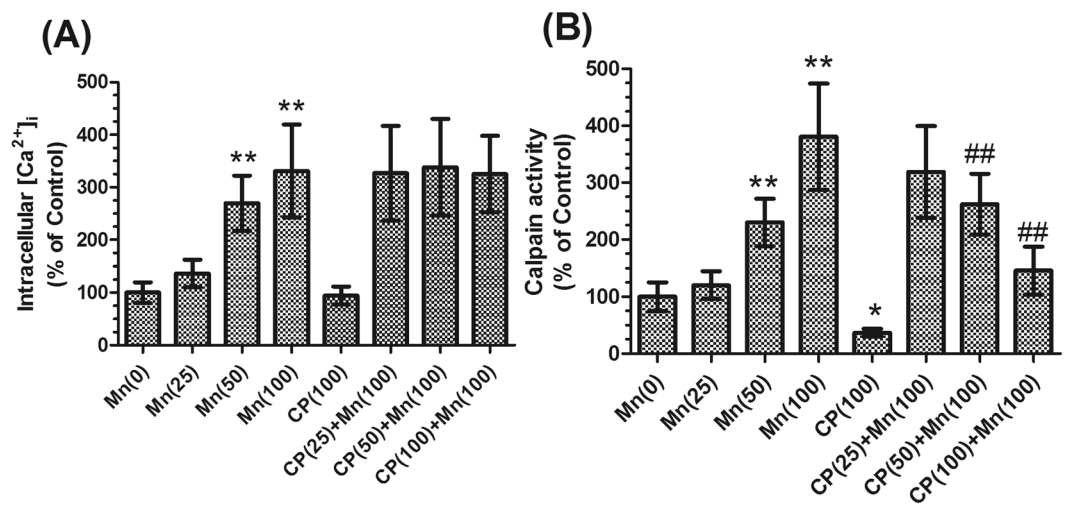


Figure 3. Effects of Mn and calpeptin pretreatment on intracellular Ca^{2+} and calpain activity in basal nuclei of mice. (A) $[\text{Ca}^{2+}]_i$ in the mice basal nuclei was calibrated from the measured fluorescence signals by the use of an F-4500 Fluorescence Spectrophotometer as described in the experimental section. (B) After brain was homogenized, calpain activity was measured using a spectrophotometer at 595 nm as described in the experimental section. Data are expressed as a percentage of controls, the values are expressed as means \pm S.D., $n = 6$. * $P < 0.05$ and ** $P < 0.01$, significantly different from control group; ## $P < 0.01$, significantly different from 100 $\mu\text{mol/kg}$ MnCl_2 -treated group.

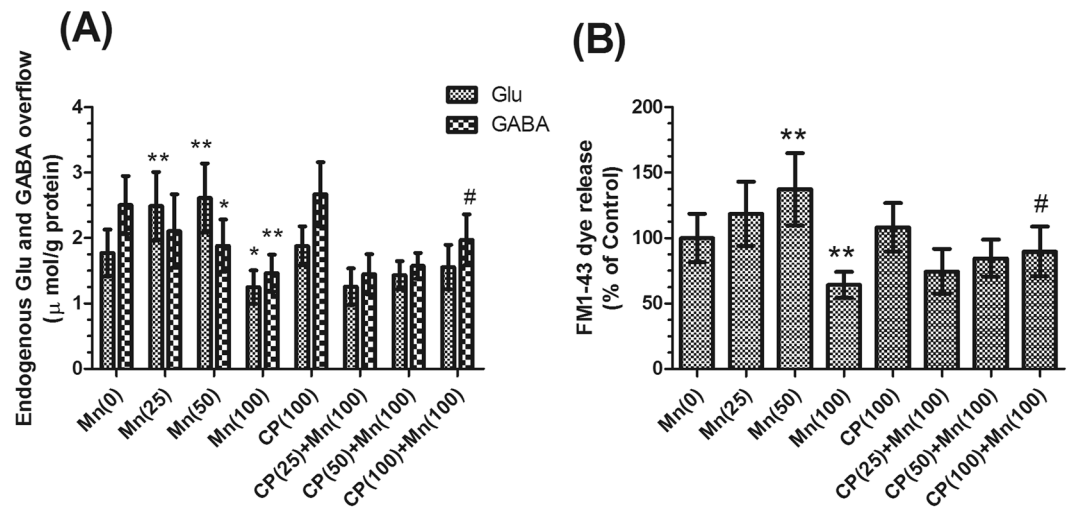


Figure 4. Calpeptin abated the Mn-induced decrease of neurotransmitters release. **(A)** Effects of MnCl₂ and calpeptin pre-treatment on Glu and GABA release in basal nuclei by using HPLC. **(B)** Effects of MnCl₂ and calpeptin pre-treatment on neurotransmitter release by using release of the fluorescent dye FM1-43. Data are expressed as a percentage of controls, the values are expressed as means ± S.D., n = 6. **P* < 0.05 and ***P* < 0.01 significantly different from control group; #*P* < 0.05, significantly different from 100 μmol/kg MnCl₂-treated group.

the N-terminus of SNAP-25 (Synaptic Systems, N-terminal) and a polyclonal antibodies against the C-terminus of SNAP-25 (Synaptic Systems, C-terminal). The expression of the N-terminus of SNAP-25 decreased significantly in 25, 50 and 100 μmol/kg MnCl₂-treated group (30.36%, 38.73% and 50.50% respectively, *P* < 0.01). However, pretreatment with 100 μg/kg calpeptin caused an increase in the expression of N-terminus of SNAP-25 compared with 100 μmol/kg MnCl₂-treated group (1.63-fold of 100 μmol/kg MnCl₂-treated group, *P* < 0.05). The expression of the C-terminus of SNAP-25 have a marked decrease in 50 and 100 μmol/kg MnCl₂-treated group (44.36% and 50.78% respectively, *P* < 0.01). However, pretreatment with 50 and 100 μmol/kg calpeptin caused an increase in the expression of C-terminus of SNAP-25 compared with 100 μmol/kg MnCl₂-treated group (1.68- and 1.87-fold of 100 μmol/kg MnCl₂-treated group, *P* < 0.05 and *P* < 0.01, respectively). However, the proteins expression of Syntaxin 1 did not have significantly change in MnCl₂-treated groups as well as calpeptin pretreated groups.

Effects of Mn and calpeptin pretreatment on the SNARE complex formation. To assess whether the number of SNARE core complexes was decreased in synaptic membranes of MnCl₂-treated mice, we measured the amount of complexes, which were detected by loading not boiled synaptic membrane proteins on 4–20% gradient gels and developing Western blots with Syntaxin 1 antibody¹⁷. Two major syntaxin-1-containing complexes, migrating at 100 kDa and 80 kDa were detected (Fig. 5A). The 25 and 50 μmol/kg MnCl₂-treated groups caused a significant increase in 80 kDa proteins levels of SNARE complexes versus controls (2.81- and 2.86-fold respectively, *P* < 0.01), and decreased by 15.18% (*P* < 0.05) in the 100 μmol/kg MnCl₂-treated group. The 80 kDa protein in calpeptin pre-treated groups did not significant change, compared with 100 μmol/kg MnCl₂-treated group (Fig. 5D). The 100 kDa protein levels of SNARE complexes did not significantly change in MnCl₂-treated groups, compared with control group. The 50 and 100 μg/kg calpeptin pre-treated groups caused a significant increase in 100 kDa proteins versus 100 μmol/kg MnCl₂-treated group (1.62- and 1.70-fold of 100 μmol/kg MnCl₂-treated group, respectively, *P* < 0.01, Fig. 5D).

Discussion

Our study has attempted to evaluate that Mn induced the disorder of neurotransmitter release through influencing the formation of SNARE complex via cleaving SNAP-25 by overactivation of calpains in basal nuclei, which is critical for evaluating the Mn-induced neurotoxicity.

In our mouse model of manganese, there were significant increase in Mn concentrations in the basal nuclei of both Mn-treated and calpeptin pre-treated mice compared with controls. To further confirm irreversible neurodegeneration and facilitate quantification following Mn intoxication, behavior was assessed by an open field test. In the present study, Mn-exposed mice were anxiety during the exploratory behavior in open field test. The locomotor activity during open field test in rodents is generally regarded as an indicator of emotional response to an unfamiliar environment, with an assumption that reduction in activity correlates with increased anxiety¹⁸. Given the results demonstrated in our study, it could be inferred that Mn exposure produced emotional alterations. Moreover, the decreased time spent in the center of the open field area indicates an increased anxiety level induced by Mn exposure. Mn-exposed mice also exhibited significant decrease in average velocity, this result suggested impairment in locomotion or emotional alterations. The increased anxiety in the face of increased depressive behavior exhibited by the Mn-exposed mice is likely related to the Mn-caused neurotransmitter release disorder¹⁹, as we discuss in more detail later.

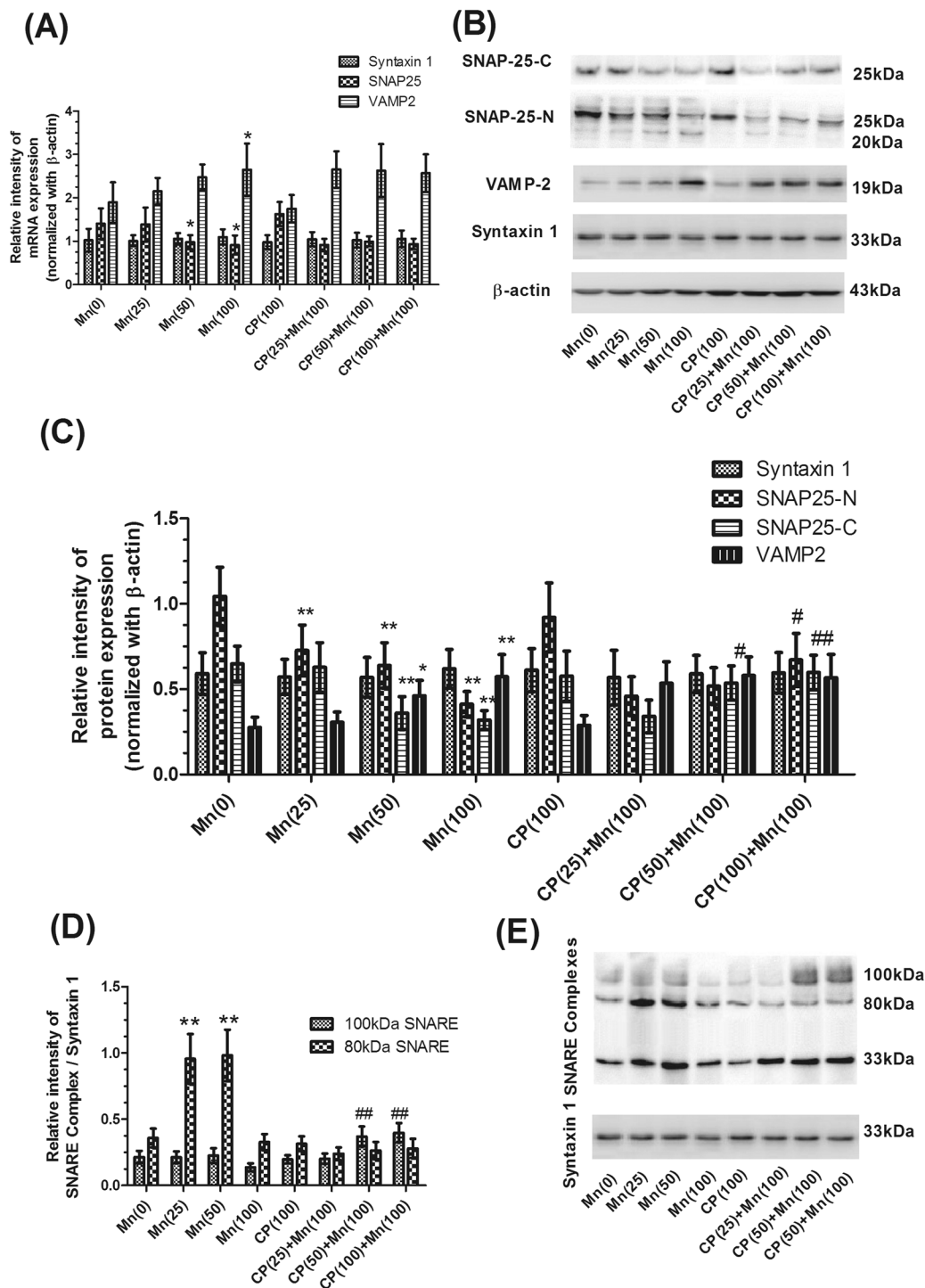


Figure 5. Calpeptin abated Mn disturbed the expression of SNARE complex associated proteins and the down-regulation of SNARE complex formation. **(A)** The mRNA expression levels were analyzed using a real-time RT-PCR assay to measure the expression of Syntaxin 1, SNAP-25 and VAMP-2 gene. Expression of Syntaxin 1, SNAP-25 and VAMP-2 gene were normalized with β -actin gene. For relative quantification of the tested, we used the comparative CT method ($\Delta\Delta$ CT). **(B)** The western blotting products of Syntaxin 1, N-terminal of SNAP-25, C-terminal of SNAP-25, VAMP-2 and β -actin. **(C)** Semi-quantitative analysis of the protein expressions of Syntaxin 1, N-terminal of SNAP-25, C-terminal of SNAP-25 and VAMP-2 were shown. Expression of Syntaxin 1, SNAP-25 and VAMP-2 protein were normalized with β -actin protein. **(D)** Semi-quantitative analysis of the protein expressions of SNARE complex protein was shown. Expression of SNARE complex protein was normalized with Syntaxin 1 protein. **(E)** The western blotting products of SNARE complex protein. Data are expressed as a percentage of controls, the values are expressed as means \pm S.D., $n = 6$. * $P < 0.05$, ** $P < 0.01$ significantly different form control group, # $P < 0.05$, ## $P < 0.01$ significantly different form 100 μ mol/kg $MnCl_2$ -treated group.

Neurotransmitter release relies on the number of available synaptic vesicles and the release probability. Accordingly, the principal ultrastructural alterations produced by the neurotoxic effect of Mn in basal nuclei were the decrease in the number of synaptic vesicles and the increase in the thickness of PSD²⁰. FM1-43 provides quantitative information about recycling pools of vesicles²¹. Our study provided evidence that the treatment with Mn resulted in synaptic vesicle fusion increasing in low dosage and decreasing in high dosage. Multiple studies have demonstrated the effect of Mn overexposure on neurotransmitter systems, like GABA and Glu²². Hence, we assessed the effect of Mn exposure on the GABA and Glu release, and found that Glu released was increased in low Mn dosage but decreased in high dosage, which was consistent with the quantity of synaptic vesicle fusion, and GABA released was decreased with Mn exposure in synaptosomes. These findings lend more support to the notion that the neurotransmitter release may be the major driving force for the Mn-induced behavioral alterations observed in this study.

Indeed, the SNARE complex and associated proteins play a critical role in vesicle docking, priming, fusion and synchronization of neurotransmitter release at presynaptic membranes and it was established that the SNARE complex corresponds to the minimal machinery for membrane fusion in eukaryotic cells, forming a stable complex that make the vesicles competent for fusion²³. Therefore, a variation of SNARE complex accumulation in synaptic membranes is connected with disorder of neurotransmitter vesicle release. Syntaxin 1, SNAP-25 and VAMP-2 proteins are all SNARE proteins which exist in all types of synapses and play a central role in the release of neurotransmitters by synaptic vesicle exocytosis¹¹. However, our study provided evidence that the treatment with Mn resulted in a dose-dependent decrease in the expression of SNAP-25 and increase in the expression of VAMP-2 but did not modify the mRNA and proteins expression of Syntaxin 1. The three proteins arrange as a tightly twisted, supercoiled, four-helical bundle with VAMP-2 anchoring in the vesicular membrane and SNAP-25 and Syntaxin 1 in the plasma membrane. The highly controlled interaction between vesicular and plasma membrane proteins is achieved by the formation of the ternary SNARE complex.

Calpains cleaves various types of presynaptic proteins: vesicular glutamate transporters, glutamatergic presynaptic sites²⁴; GABAergic presynaptic sites such as glutamic acid decarboxylase, vesicular GABA transporter; plasma membrane GABA transporters²⁵; and other important presynaptic proteins, such as synaptophysin and SNAP-25²⁶. Numerous studies have shown presynaptic effects of calpains on glutamatergic and GABAergic synapses, targeting membrane-associated proteins as well as intracellular proteins. The resulting changes in the presynaptic proteome alter neurotransmitter release. These alterations also disturb the balance between excitatory and inhibitory neurotransmission in the brain²⁷. Previous studies have found that the calpains cleavage site in SNAP-25 should be located at the C-terminal side¹⁶, thus proteins tested by C-terminal antibodies represent the full length of SNAP-25, and proteins tested by N-terminal antibodies are N-terminal fragments of SNAP-25. In the present study, treatment with Mn caused N-terminal fragments of SNAP-25 appeared and significant decrease in the number of SNAP-25. Strikingly, compared with 100 $\mu\text{mol/kg}$ Mn-treated groups, there was a significant increase in the full length of SNAP-25 and N-terminal fragments were disappeared in 100 μM calpeptin pre-treated mice, which could be explained by inhibited calpains activity.

Calpains are upregulated in a wide range of pathophysiological conditions characterized by dysregulation of neuronal calcium homeostasis, including stroke, epilepsy, traumatic brain injury and neurodegenerative disorders^{28, 29} and they are, indeed, recognized to be important mediators of neurotransmitter release disorder³⁰. Small calcium changes falling into the physiological range can already result in significant variations of calpains activity¹⁵. Once they are activated by increased cytosolic Ca^{2+} load, calpains degrade a large number of cellular proteins, including SNAP-25 protein ultimately leading to neurotransmitter release disorder. ATP-driven plasma membrane calcium-pump (Ca^{2+} -ATPase) is of crucial importance in maintaining a low resting intracellular Ca^{2+} concentration³¹. Previous studies have indicated Mn preferentially accumulates in mitochondria, where it disrupts oxidative phosphorylation and increases the generation of reactive oxygen species (ROS)³². Furthermore, it has been demonstrated that ROS overproduction might inhibit Ca^{2+} -ATPases and this leads to altered regulation of Ca^{2+} levels³³. Therefore, the inhibitory effect of Mn^{2+} on Ca^{2+} -ATPases might be one of the reasons that causes a significant increase of $[\text{Ca}^{2+}]_i$ in neuron. Our previous studies also have found that overactivation of N-methyl-D-aspartate receptors (NMDARs), a phenomenon known as excitotoxicity, by Mn could result in an influx of extracellular Ca^{2+} , which triggers a series of toxic events³⁴. In addition to the inflow of extracellular calcium can lead to increased $[\text{Ca}^{2+}]_i$, endoplasmic reticulum(ER) stress can also lead to that. Our previous study have reported that Mn could induce ER stress³⁵. Nearly 30% of proteins are not folded properly and misfolded proteins are retained in the ER, translocated to cytoplasm and degraded by proteasome (ER associated degradation). An abnormal protein burden in ER can lead to release of intracellular Ca^{2+} from ER, leading to mitochondrial Ca^{2+} uptake³⁶. In this study, *in vivo* treatment of mice with Mn resulted in a significant increase in $[\text{Ca}^{2+}]_i$ and the activity of calpains. The results showed that calpains activity was excessively activated by Mn. It has been shown that the calpain-mediated SNAP-25 fragmentation correlates with a reduction of the SNARE function and inhibition of neurotransmitter release.

Calpeptin, an inhibitor of calpains, was used in this study. Therefore, our results demonstrated that calpeptin pretreatment significantly decreased in calpains activity, as well as partially increased SNARE complex protein formation. Moreover, there was none N-terminal of SNAP-25 in 100 $\mu\text{g/kg}$ calpeptin pre-treated group. To confirm that calpeptin is non-toxic in low doses, we designed the present study to include a calpeptin alone group. The results demonstrated that there were no statistically significant differences in mice that were treated with calpeptin alone compared with controls. Based on these results, we concluded that low doses of calpeptin not only could inhibit the pathological consequences of calpains overactivation but also preserve cleavage of SNAP-25.

Taken together, the results of this study showed that Mn induced the disorder of neurotransmitter release through influencing the formation of SNARE complex via cleaving SNAP-25 by excessive activation of calpains *in vivo*. Moreover, inhibition of calpains could partially inhibit Mn-induced neurotransmitter release disorder. Our

results give insight into the neurochemical alterations that take place in basal nuclei during elevated Mn exposure, and inhibition of calpains may represent a novel therapeutic target to ameliorate neuronal damage in manganism.

Material and Methods

Material. Manganese (II) chloride tetrahydrate ($\text{MnCl}_2 \cdot 4\text{H}_2\text{O}$), Calpains, Calpeptin, SynaptoGreenTMC4 (FM1-43) and L-glutamine were purchased from Sigma (Saint Louis, MO, USA). PrimeScript[®]RT Enzyme Mix I and SYBR[®]Premix Ex TaqTMII kits were from TaKaRa Biotech. Co. Ltd. Mouse β -actin primary antibodies were purchased from Santa Cruz Biotechnology, Inc. (Santa Cruz, CA). Rabbit Syntaxin 1, VAMP-2 primary antibody were purchased from Abcam Ltd. (Hong Kong), mouse SNAP-25 N-terminal monoclonal and C-terminal polyclonal antibodies were purchased from Synaptic Systems (Germany). Horseradish peroxidase (HRP) conjugated anti-rabbit secondary antibody and HRP conjugated anti-mouse secondary antibody were purchased from Abcam. Additional chemicals of analytical grade were obtained from local chemical suppliers.

Animal Procedures. A total of 24 male and 24 female adult Kunming mice weighing 25 ± 2 g were obtained from the Laboratory Animal Center of China Medicine University (SPF grade, Certificate No. SCXK 2013-0001). They were housed under conventional conditions at a room temperature of 21–24 °C, with a 12 h light: 12 h dark cycle and humidity of 30–40%. They were permitted free access to food and water. The animal experiment was carried out according to the National Institutes of Health Guidelines for the Care and Use of Laboratory Animals and approved by the local authorities. All efforts were made to minimize the number of animals used and their suffering. The mice were randomly divided into eight groups of six mice (three male and three female): control group, MnCl_2 -exposed groups (25, 50, 100 $\mu\text{mol/kg}$), calpeptin control group, and calpeptin pre-treated groups (25, 50, 100 $\mu\text{g/kg}$). The control group mice were intraperitoneally (i.p.) injected with physiological saline (group 1). MnCl_2 -exposed mice were respectively i.p. injected with 25, 50 and 100 $\mu\text{mol/kg}$ MnCl_2 in sterile deionized water (group 2, 3, 4). The calpeptin control group mice were subcutaneously (s.c.) injected with 100 $\mu\text{g/kg}$ body weight calpeptin solution, 2 h before the i.p. administration with physiological saline (group 5). The calpeptin pre-treated mice were respectively s.c. injected with 25, 50, 100 $\mu\text{g/kg}$ calpeptin solution, 2 h before the i.p. administration with 100 μmol MnCl_2/kg bodyweight (group 6, 7, 8). The volume of injection was 2 ml/kg body weight, once every day, continuous injection for 24 days. For biochemical analysis, mice were killed by decapitation. The experimental protocols were approved by the Laboratory Animal Center of China Medicine University.

Open field test. In order to assess possible effects of drug treatment on spontaneous locomotor activity, the animals were submitted to the open field paradigm as previously described³⁷. Briefly, the open field area (50 × 50 × 50 cm) with a video camera attached to a computer was used to record animal behaviors, measured using EthoVision XT 11 software. 8, 16, 24 days after the administration, each mouse was placed individually into the center of the area and permitted free exploration. For analysis, the open field area was divided into two squares, the inner central zone (25 × 25 cm) and the outer periphery zone (25 cm from the walls). The mouse was positioned in the center of the area for 2 min to acclimatization then recorded for 5 min. The total distance traveled, average velocity and time in the inner central zone were measured respectively. Between each subject, the chambers were thoroughly cleaned and wiped down with 70% ethanol.

Measurement of Mn concentration in basal nuclei. A weighed amount of tissue was wet-digested with 500 μl HNO_3 (70% HNO_3 for trace metal analysis). After partial evaporation, samples were cooled down, 500 μl H_2O_2 (36.5–38.0% for trace metal analysis) was added and the solution was totally evaporated. The precipitate was dissolved in 5 ml deionized water and analysis was performed by a HITACHI 180–80 atomic absorption spectrophotometer. Concentrations were measured using a standard calibration curve.

Transmission Electron Microscopy. The basal nuclei specimens (1 mm³) were dissected from the basal nuclei area 25 days after drug treatment. Briefly, the samples were placed in 2.5% glutaraldehyde and post-fixed with 1% osmium tetroxide. After graded ethyl alcohols, the cubes were embedded in Epon618. Thin sections laid on copper mesh were stained with heavy metals, uranyl acetate, and lead citrate for contrast. A Hitachi-H7650 transmission electron microscope (TEM; Hitachi, Japan) was used to observe the neural synapse ultrastructure.

Measurement of intracellular free calcium. After preparation of the dissociated tissue, the $[\text{Ca}^{2+}]_i$ assay was performed by a method described previously³⁸. Briefly, for fura-2 experiments, absolute values of $[\text{Ca}^{2+}]_i$ in the neurocyte were calibrated from the measured fluorescence signals using an F-4500 Fluorescence Spectrophotometer (Hitachi, Japan). Consequences of an individual experiment are reported. Similar data were obtained in six independent experiments. The calibration equation used was: $[\text{Ca}^{2+}]_i = K_d [(R - R_{\min}) / (R_{\max} - R)] \times (S_{380} / S_{340})$. $[\text{Ca}^{2+}]_i$ is the concentration (nM) of intracellular Ca^{2+} ; K_d is the dissociation constant of the dye; R is the ratio at excitation wavelengths 340/380 nm; R_{\min} is the ratio at zero $[\text{Ca}^{2+}]_i$; and R_{\max} is the ratio at saturated $[\text{Ca}^{2+}]_i$. The procedures for obtaining R_{\max} and R_{\min} caused damage to cells and were therefore performed at the end of the experiments. R_{\max} was obtained first by adding Triton X-100 (0.2%), making the cell membrane permeable to Ca^{2+} and allowing the extracellular and intracellular Ca^{2+} to equilibrate. Next, R_{\min} was obtained by adding the chelator EGTA [ethylene glycol bis (β -aminoethyl ether)-N, N, N', N'-tetraacetic acid; 20 mM] to chelate all Ca^{2+} inside and outside the cells. The present experiments were carried out at pH 7.4 and a temperature of 37 °C. A K_d value of 224 nM was used. The results are expressed as a percentage of the controls.

Measurement of calpains activity. Calpains activity was assayed as described by Buroker-Kilgore and Wang³⁹. Briefly, after the brain tissues were homogenized in an extraction medium containing 5 mM β -mercaptoethanol, 0.1 mM EDTA, lysocephalin 5 mM, DL-Dithiothreitol 10 mM and 20 mM Tris-HCl at pH

8.6, tissue homogenate was centrifuged at $1000\times g$ for 10 min to remove the protein precipitate. Samples were incubated with the calpains substrate casein, and after removal of an aliquot, Coomassie brilliant blue G-250 dye reagent was added to the aliquot and was quantified using a spectrophotometer at 595 nm. Calpains activity was calculated as the difference between samples with and without Ca^{2+} . The results are expressed as a percentage of the controls.

Preparation of synaptosomes from mice brain. Percoll-purified synaptosomes were prepared using the basal nuclei of mice, as described previously⁴⁰. The mice were killed by decapitation, and the basal nuclei were rapidly removed at 4 °C. Synaptosomes were prepared by Percoll density-gradient centrifugation techniques. Briefly, the basal nuclei was isolated and homogenized in a medium that contained 320 mM sucrose, pH 7.4. The homogenate was centrifuged at 3000 g (5000 rpm in a JA 25.5 rotor; Beckman Coulter, Inc., USA) for 10 min at 4 °C, and the supernatant was centrifuged again at 14,500 g (11,000 rpm in a JA 25.5 rotor) for 12 min at 4 °C. The pellet was gently resuspended in 8 ml of 320 mM sucrose, pH 7.4. Two milliliters of this synaptosomal suspension was placed into 3 ml Percoll discontinuous gradients containing 320 mM sucrose, 1 mM EDTA, 0.25 mM DL-dithiothreitol, and 3, 10 and 23% Percoll, pH 7.4. The gradients were centrifuged at 32,500 g (16,500 rpm in a JA 20.5 rotor) for 7 min at 4 °C. Synaptosomes sedimenting between the 10 and the 23% Percoll bands were collected and diluted in a final volume of 30 ml of HEPES buffer medium (HBM) consisting of 140 mM NaCl, 5 mM KCl, 5 mM $NaHCO_3$, 1 mM $MgCl_2\cdot 6H_2O$, 1.2 mM Na_2HPO_4 , 10 mM glucose, and 10 mM HEPES (pH 7.4). Protein concentration was determined using the Bradford assay. Synaptosomes were centrifuged in the final wash to obtain synaptosomal pellets with 0.5 mg protein. The synaptosomal pellets were stored on ice and used within 4–6 h.

FM1-43 fluorescence image analysis. Synaptic vesicle fusion with the plasma membrane was measured using release of the fluorescent dye FM1-43, as described previously⁴¹. In brief, synaptosomes (0.5 mg/ml) were incubated in HBM with 1.2 mM $CaCl_2$ for 2 min at 37 °C in a stirred test tube. FM1-43 (100 μM) was added 1 min before stimulation with 30 mM KCl. After 3 min of stimulation to load FM1-43, synaptosomes were washed twice in HBM that contained 1.2 mM $CaCl_2$ and 1 mg/ml BSA to remove non-internalized FM1-43. Synaptosomes were then resuspended in 2 ml of HBM (plus 1.2 mM Ca^{2+}), and incubated in a stirred and thermostated cuvette maintained at 37 °C in a Perkin-Elmer LS-50B spectrofluorimeter. Release of accumulated FM1-43 was induced by the addition of 30 mM KCl, and measured as the decrease in fluorescence upon release of the dye into solution (excitation 488 nm, emission 540 nm). Data points were obtained at 2-s intervals, and data presented as the Ca^{2+} -dependent decrease in FM1-43 fluorescence. Any drugs were added after the dye-loading procedure, and the synaptosomes were preincubated with osthole or imperatorin for 10 min before depolarization with KCl.

Endogenous Glu and GABA release. Endogenous neurotransmitter release was measured as previously reported^{42,43}. Synaptosomes (about 100 μg of protein) were layered on microporous filters at the bottom of a set of parallel superfusion chambers maintained at 37 °C. A 30-min period of stimulation was applied with 15 mM KCl substituting for an equimolar concentration of NaCl. Fractions collected were analyzed for endogenous Glu and GABA content. Amino acid release was expressed as $\mu mol/g$ of protein. Endogenous Glu and GABA were measured by High Performance Liquid Chromatography (HPLC) analysis after precolumn derivatization with o-phthalaldehyde and separation on a ZORBAX Eclipse XDB-C18 reverse-phase chromatographic column (250 \times 4.6 mm, 5 μm ; at 30 °C; Agilent Technologies, USA) coupled with fluorometric detection (excitation wavelength, 250 nm; emission wavelength, 410 nm). Buffers and the gradient program were as follows: solvent A, methanol; solvent B, 0.1 M sodium acetate (pH 5.8); gradient program, 20% A for 2 min from the initiation of the program; 47% A in 2 min; isocratic flow, 7 min; 53% A in 9 min; isocratic flow, 3 min; 100% A in 12 min; isocratic flow, 6 min; flow rate, 1.0 ml/min.

Quantitative real-time PCR analysis. The mRNA expression levels were analyzed using a real-time reverse-transcription polymerase chain reaction assay. Total RNA was isolated using TRIzol reagent (TaKaRa Biotech. Co. Ltd., China). The first strand cDNA was synthesized from 1 μg of total RNA by reverse transcriptase using PrimeScript[®] RT Enzyme Mix I (TaKaRa Biotech. Co. Ltd., China) and oligo (dT) primers according to the manufacturer's protocol. Real-time quantitative PCR (qPCR) was performed by SYBR[®] Premix Ex Taq[™] II kit (TaKaRa Biotech. Co. Ltd., China) using an ABI 7500 Real-Time PCR System (Applied Biosystems, USA). Two microliters of template cDNA was added to the final volume of 20 μl of reaction mixture. Real-time PCR cycle parameters were 30 sec at 95 °C followed by 40 cycles with denatured at 95 °C for 5 sec, annealing at 60 °C for 34 sec and elongating at 72 °C for 20 sec. There are the sequences of the specific primer sets: Syntaxin 1's Sense primer is 5'-ACCGCTTCATGGATGAGTTC-3' and Anti-sense primer is 5'-GAGCTCCTCCAGTTCCTCCT-3', SNAP-25's Sense primer is 5'-CTGGCATCAGGACTTTGGTT-3' and Anti-sense primer is 5'-ATTATGCCCCAGGCTTTT-3', VAMP-2's Sense primer is 5'-CTGCACCTCCTCCAAATCTT-3' and Anti-sense primer is 5'-CTTGCTGCACTTGTTCAA-3', β -actin's Sense primer is 5'-GGAGATTACTGCCCTGGCTCCTA-3' and Anti-sense primer is 5'-GGAGATTACTGCCCTGGCTCCTA-3²⁰. Expressions of selected genes were normalized with the gene for β -actin, which was used as an internal housekeeping control. For relative quantification of the genes tested, we used the comparative CT method ($\Delta\Delta CT$). All the real-time PCR experiments were performed in quadruplicate, and data were expressed as the mean of at least four independent experiments.

Western blotting. Samples of each fraction were analyzed by SDS-PAGE followed by Western blot. Tissue were rinsed with PBS and total protein was extracted from the neurons using RIPA buffer (10 mM Na_2HPO_4 , pH 7.2, 150 mM NaCl, 1% sodium deoxycholate, 1% Nonidet P-40, 0.1% SDS) containing protease inhibitors (1 mM phenylmethylsulfonyl fluoride, 0.2 mM 1, 10-phenanthroline, 10 $\mu g/ml$ pepstatin A, 10 $\mu g/ml$ leupeptin, 10 $\mu g/ml$

mL aprotinin, and 10 mM benzamidine). Protein concentrations were determined with the BCA reagent from Pierce. Equal amounts of protein (20 µg) were separated by 10% polyacrylamide gel electrophoresis and transferred to polyvinylidene difluoride (PVDF) membranes (Millipore, Tercinula, CA). PVDF membranes blocked overnight at 4 °C in TBST containing 5% bovine serum albumin fraction V. Following which, the membranes were rinsed briefly in TBST and incubated with primary antibody in TBST for a night at 4 °C. Single components of SNARE were detected by incubated with Syntaxin 1 (1:200), VAMP-2 (1:200) and β-actin (1:200). SNAP-25 cleavage products were detected by incubating filters in anti-SNAP-25 N-terminal monoclonal (directed against the epitope containing amino acid residues 1–20) and C-terminal polyclonal antibodies (directed against AAs 192–206) (1:1000; Synaptic Systems, Germany). Specific protein expression was then detected by incubating the washed membranes with HRP conjugated secondary antibodies (1:2000). Protein bands were visualized by using the ECL Western blotting chemiluminescent detection reagents and autoradiography. The intensity of the bands was evaluated semi-quantitatively by densitometry using image analyzing software (FluorChem v2.0). The changes of intensity of Syntaxin 1, VAMP-2, anti-SNAP-25 N-terminal monoclonal and C-terminal polyclonal antibodies proteins after MnCl₂ treatment were normalized using the intensity obtained in the internal control bands (β-actin). Results of an individual experiment that reflects similar data obtained on at least three separate occasions.

SNARE complex analysis. For detection of SDS-resistant SNARE complexes, Western blotting was performed on samples of electrophoresed protein extraction (non-boiled before gel loading)¹⁷, incubating PVDF membranes containing blotted proteins with rabbit polyclonal antibodies for Syntaxin 1 (1:1000). The membranes were incubated with anti-rabbit secondary antibody (1:2000), and immunoreactive bands visualized by chemiluminescent detection reagents (Pierce). All bands were normalized with Syntaxin 1 monomer level (normal Western blotting) in the same sample.

Statistical analysis. Statistical analyses were performed using SPSS 18.0 and the results were expressed as the mean ± S.D. Differences between the means were determined by one-way ANOVA followed by a Student–Newman–Keuls test for multiple comparisons. The difference at either $P < 0.05$ or $P < 0.01$ was considered statistically significant.

References

- Oulhote, Y. *et al.* Neurobehavioral function in school-age children exposed to manganese in drinking water. *Environ Health Perspect* **122**, 1343–1350 (2014).
- Nookabkaew, S. *et al.* Evaluation of trace elements in selected foods and dietary intake by young children in Thailand. *Food Addit Contam Part B Surveill* **6**, 55–67 (2013).
- Finkelstein, M. M. & Jerrett, M. A study of the relationships between Parkinson's disease and markers of traffic-derived and environmental manganese air pollution in two Canadian cities. *Environmental Research* **104**, 420–432 (2007).
- Gonzalez-Cuyar, L. F. *et al.* Quantitative neuropathology associated with chronic manganese exposure in South African mine workers. *Neurotoxicology* **45**, 260–266 (2014).
- Cordova, F. M. *et al.* Manganese-exposed developing rats display motor deficits and striatal oxidative stress that are reversed by Trolox. *Archives of Toxicology* **87**, 1231–1244 (2013).
- Martinez-Finley, E. J., Gavin, C. E., Aschner, M. & Gunter, T. E. Manganese neurotoxicity and the role of reactive oxygen species. *Free Radical Biology and Medicine* **62**, 65–75 (2013).
- Sidoryk-Wegrzynowicz, M. & Aschner, M. Role of astrocytes in manganese mediated neurotoxicity. *BMC Pharmacol Toxicol* **14**, 23 (2013).
- Moberly, A. H. *et al.* Intranasal exposure to manganese disrupts neurotransmitter release from glutamatergic synapses in the central nervous system *in vivo*. *Neurotoxicology* **33**, 996–1004 (2012).
- Takeda, A., Sotogaku, N. & Oku, N. Manganese influences the levels of neurotransmitters in synapses in rat brain. *Neuroscience* **114**, 669–674 (2002).
- Lee, E. S. Y., Sidoryk, M., Jiang, H. Y., Yin, Z. B. & Aschner, M. Estrogen and tamoxifen reverse manganese-induced glutamate transporter impairment in astrocytes. *Journal of Neurochemistry* **110**, 530–544 (2009).
- Shin, O. H. Exocytosis and synaptic vesicle function. *Compr Physiol* **4**, 149–175 (2014).
- Fang, Q. H. & Lindau, M. How Could SNARE Proteins Open a Fusion Pore? *Physiology* **29**, 278–285 (2014).
- Sudhof, T. C. & Rizo, J. Synaptic Vesicle Exocytosis. *Cold Spring Harbor Perspectives in Biology* **3**, doi:10.1101/cshperspect.a005637, (2011).
- Wang, C. *et al.* Manganese exposure disrupts SNARE protein complex-mediated vesicle fusion in primary cultured neurons. *Environ Toxicol*, doi:10.1002/tox.22272 (2016).
- Grumelli, C. *et al.* Calpain activity contributes to the control of SNAP-25 levels in neurons. *Mol Cell Neurosci* **39**, 314–323 (2008).
- Ando, K., Kudo, Y. & Takahashi, M. Negative regulation of neurotransmitter release by calpain: a possible involvement of specific SNAP-25 cleavage. *Journal of Neurochemistry* **94**, 651–658 (2005).
- Musazzi, L. *et al.* Acute Stress Increases Depolarization-Evoked Glutamate Release in the Rat Prefrontal/Frontal Cortex: The Dampening Action of Antidepressants. *Plos One* **5**, doi:ARTN e856610.1371/journal.pone.0008566, (2010).
- Neto, J. D. N. *et al.* Antioxidant Effects of Nerolidol in Mice Hippocampus After Open Field Test. *Neurochemical Research* **38**, 1861–1870 (2013).
- Krishna, S., Dodd, C. A., Hekmatyar, S. K. & Filipov, N. M. Brain deposition and neurotoxicity of manganese in adult mice exposed via the drinking water. *Arch Toxicol* **88**, 47–64 (2014).
- Elfving, B., Bonefeld, B. E., Rosenberg, R. & Wegener, G. Differential expression of synaptic vesicle proteins after repeated electroconvulsive seizures in rat frontal cortex and hippocampus. *Synapse* **62**, 662–670 (2008).
- Shinoda, Y. *et al.* BDNF enhances spontaneous and activity-dependent neurotransmitter release at excitatory terminals but not at inhibitory terminals in hippocampal neurons. *Front Synaptic Neurosci* **6**, 27 (2014).
- Burton, N. C., Schneider, J. S., Syversen, T. & Guilarte, T. R. Effects of Chronic Manganese Exposure on Glutamatergic and GABAergic Neurotransmitter Markers in the Nonhuman Primate Brain. *Toxicological Sciences* **111**, 131–139 (2009).
- Sudhof, T. C. Neurotransmitter Release: The Last Millisecond in the Life of a Synaptic Vesicle. *Neuron* **80**, 675–690 (2013).
- Foss, S. M., Li, H., Santos, M. S., Edwards, R. H. & Voglmaier, S. M. Multiple dileucine-like motifs direct VGLUT1 trafficking. *J. Neurosci* **33**, 10647–10660 (2013).

25. Gomes, J. R. *et al.* Cleavage of the vesicular GABA transporter under excitotoxic conditions is followed by accumulation of the truncated transporter in nonsynaptic sites. *J. Neurosci* **31**, 4622–4635 (2011).
26. Grumelli, C. *et al.* Calpain activity contributes to the control of SNAP-25 levels in neurons. *Mol. Cell. Neurosci* **39**, 314–323 (2008).
27. Baudry, M. & Bi, X. Calpain-1 and calpain-2: the yin and yang of synaptic plasticity and neurodegeneration. *Trends Neurosci* **39**, 235–245 (2016).
28. Sun, D. A., Sombati, S., Blair, R. E. & DeLorenzo, R. J. Long-lasting alterations in neuronal calcium homeostasis in an *in vitro* model of stroke-induced epilepsy. *Cell Calcium* **35**, 155–163 (2004).
29. Tyagarajan, S. K. *et al.* Extracellular signal-regulated kinase and glycogen synthase kinase 3 β regulate gephyrin postsynaptic aggregation and GABAergic synaptic function in a calpain-dependent mechanism. *J Biol Chem* **288**, 9634–9647 (2013).
30. Neumar, R. W., Xu, Y. A., Gada, H., Guttmann, R. P. & Siman, R. Cross-talk between calpain and caspase proteolytic systems during neuronal apoptosis. *Journal of Biological Chemistry* **278**, 14162–14167 (2003).
31. Szymraj, J., Kawecka, I., Bartkowiak, J. & Zylinska, L. The effect of antisense oligonucleotide treatment of plasma membrane Ca²⁺-ATPase in PC12 cells. *Cell Mol Biol Lett* **9**, 451–464 (2004).
32. Gunter, T. E., Gavin, C. E., Aschner, M. & Gunter, K. K. Speciation of manganese in cells and mitochondria: a search for the proximal cause of manganese neurotoxicity. *Neurotoxicology* **27**, 765–776 (2006).
33. Baggaley, E. M., Elliott, A. C. & Bruce, J. I. Oxidant-induced inhibition of the plasma membrane Ca²⁺-ATPase in pancreatic acinar cells: role of the mitochondria. *Am J Physiol Cell Physiol* **295**, C1247–1260 (2008).
34. Xu, B., Xu, Z. F. & Deng, Y. Effect of manganese exposure on intracellular Ca²⁺ homeostasis and expression of NMDA receptor subunits in primary cultured neurons. *Neurotoxicology* **30**, 941–949 (2009).
35. Bin Xu. *et al.* Alpha-Synuclein is Involved in Manganese-Induced ER Stress via PERK Signal Pathway in Organotypic Brain Slice Cultures. *Mol Neurobiol* **49**, 399–412 (2014).
36. Honma Y. *et al.* Trehalose activates autophagy and decreases proteasome inhibitor-induced endoplasmic reticulum stress and oxidative stress-mediated cytotoxicity in hepatocytes. *Hepatal Res.* doi:10.1111/hepr.12892 (2017).
37. Alberry, B. & Singh, S. M. Developmental and behavioral consequences of early life maternal separation stress in a mouse model of fetal alcohol spectrum disorder. *Behavioural Brain Research* **308**, 94–103 (2016).
38. He, Y. *et al.* Prolonged exposure of cortical neurons to oligomeric amyloid-beta impairs NMDA receptor function via NADPH oxidase-mediated ROS production: protective effect of green tea (–)-epigallocatechin-3-gallate. *Asn Neuro* **3**, 13–24 (2011).
39. Buroker-Kilgore, M. & Wang, K. K. A Coomassie brilliant blue G-250-based colorimetric assay for measuring activity of calpain and other proteases. *Anal Biochem* **208**, 387–392 (1993).
40. Nicholls, D. G. & Sihra, T. S. Synaptosomes possess an exocytotic pool of glutamate. *Nature* **321**, 772–773 (1986).
41. Baldwin, M. L., Rostas, J. A. & Sim, A. T. Two modes of exocytosis from synaptosomes are differentially regulated by protein phosphatase types 2A and 2B. *J Neurochem* **85**, 1190–1199 (2003).
42. Bonanno, G. *et al.* Chronic antidepressants reduce depolarization-evoked glutamate release and protein interactions favoring formation of SNARE complex in hippocampus. *J Neurosci* **25**, 3270–3279 (2005).
43. Milanese, M. *et al.* Chronic treatment with agomelatine or venlafaxine reduces depolarization-evoked glutamate release from hippocampal synaptosomes. *BMC Neurosci* **14**, 75 (2013).

Acknowledgements

This work was supported by grants from the National Natural Science Foundation of China (Grant no. 81372942); the programs for Liaoning Excellent Talents in University (Grant no. LJQ014089) and Liaoning Innovative Research Team in University (LT2015028).

Author Contributions

C.W., Z.M. and C.L. carried out the experiments and data analyses. W.L. and Y.D. prepared figures, B.X. designed the study, Z.F.X. supervised the data, and C.W. wrote the manuscript. All authors approved the final manuscript.

Additional Information

Competing Interests: The authors declare that they have no competing interests.

Publisher's note: Springer Nature remains neutral with regard to jurisdictional claims in published maps and institutional affiliations.



Open Access This article is licensed under a Creative Commons Attribution 4.0 International License, which permits use, sharing, adaptation, distribution and reproduction in any medium or format, as long as you give appropriate credit to the original author(s) and the source, provide a link to the Creative Commons license, and indicate if changes were made. The images or other third party material in this article are included in the article's Creative Commons license, unless indicated otherwise in a credit line to the material. If material is not included in the article's Creative Commons license and your intended use is not permitted by statutory regulation or exceeds the permitted use, you will need to obtain permission directly from the copyright holder. To view a copy of this license, visit <http://creativecommons.org/licenses/by/4.0/>.

© The Author(s) 2017